

Improving the Level of Autism Discrimination through GraphRNN Link Prediction

Haonan Sun^{a,1}, Qiang He^{a,2}, Shouliang Qi^{a,3}, Yudong Yao^{c,4} and Yueyang Teng^{a,b,*,5}

^aCollege of Medicine and Biological Information Engineering, Northeastern University, 110004 Shenyang, China

^bKey Laboratory of Intelligent Computing in Medical Image, Ministry of Education, Northeastern University, 110169 Shenyang, China

^cDepartment of Electrical and Computer Engineering, Stevens Institute of Technology, Hoboken, NJ, USA

ARTICLE INFO

Keywords:

Autism
Classification
Data Augmentation
Functional Connectivity
GraphRNN
Link Prediction

ABSTRACT

Dataset is the key of deep learning in Autism disease research. However, due to the few quantity and heterogeneity of samples in current dataset, for example ABIDE (Autism Brain Imaging Data Exchange), the recognition research is not effective enough. Previous studies mostly focused on optimizing feature selection methods and data reinforcement to improve accuracy. This paper is based on the latter technique, which learns the edge distribution of real brain network through GraphRNN, and generates the synthetic data which has incentive effect on the discriminant model. The experimental results show that the combination of original and synthetic data greatly improves the discrimination of the neural network. For instance, the most significant effect is the 50-layer ResNet, and the best generation model is GraphRNN, which improves the accuracy by 32.51% compared with the model reference experiment without generation data reinforcement. Because the generated data comes from the learned edge connection distribution of Autism patients and typical controls functional connectivity, but it has better effect than the original data, which has constructive significance for further understanding of disease mechanism and development.

1. Introduction

In the research of brain network science, it is extremely important to select the appropriate dataset for the computer to identify the structural anomalies correctly and efficiently (Ferrari et al., 2020). In fact, with the collaborative efforts of researchers, a lot of large datasets have been established, such as Autism Brain Imaging Data Exchange (ABIDE) (Cradock et al., 2013a; Di Martino et al., 2014) based on Autism, Alzheimer's Disease Neuroimaging Initiative (ADNI) (Petersen et al., 2010) based on Alzheimer's disease, Parkinson's Progression Markers Initiative (PPMI) (Marek et al., 2011) based on Parkinson's disease, etc. Although the data of patients with brain diseases and controls are huge, due to the large data of each individual in brain imaging. In fact, due to difficulties in collection and other reasons, the number of individual samples in the dataset cannot be as sufficient as in other fields. This leads to the direct training is difficult to fully learn the effective information (Kong et al., 2019; Xia-An et al., 2018; Xinyu et al., 2017). Therefore, the prediction model is obviously not universally applicable to individual differences. And it is easy to appear that the training accuracy is high, but it can only get a low accuracy in the test dataset (Li et al., 2018; Zhang et al., 2020).

It is worth noting that many studies (Anirudh and J. Thiagarajan, 2019; Choi, 2017; Dvornek et al.; Eslami et al., 2019; Heinsfeld et al., 2018; Khosla et al., 2018; Ktena et al., 2018; Parisot et al.; Yao et al.) in ABIDE have not achieved high accuracy in PPMI (Choi et al., 2017; Martinez-Murcia et al.; Sivaranjini and Sujatha, 2020) and ADNI (Liu et al., 2018; Lu et al., 2018; Suk et al., 2015). According to the results of previous studies, in addition to the number of sam-

ples in the dataset, it may also be due to the significant heterogeneity (Anderson et al., 2011; Frith, 2004; Hahamy et al., 2015; Just et al., 2004; Keown et al., 2013; Lawson et al., 2014; Supekar et al., 2013) of Autism (which makes it difficult to determine the appropriate classification label standard), the difficulty in distinguishing the Control group from the autistic patients after preprocessing (Kazi et al., 2018), and other factors. How to make the model from the large-scale dataset training, still has high prediction accuracy for the functional connectivity network of patients with brain disease, has been one of the key problems (Braun et al., 2018; Lanillos et al., 2020; Zhang et al., 2020).


For this reason, in previous studies, many researchers used manual (Betzel et al., 2016; Rubinov and Sporns, 2010), Autoencoder (AE) (Choi, 2017; Eslami et al., 2019) and Sparse Autoencoder (SAE) (Kong et al., 2019; Li et al., 2018; Xinyu et al., 2017) to select features. In practical terms, researchers prefer to choose features that improve the dataset, which leads to three problems:

- i) Most of the models only have high accuracy when they are trained on few datasets;
- ii) It has to identify many features by researchers;
- iii) The subjectivity of the method is relatively obvious.

We need to get a method that is generally applicable to all patients and controls brain networks:

Another idea is the augmentation of the dataset (Shorten and Khoshgoftaar, 2019; Zoph et al., 2019). It is worth noting that the traditional image data processing, such as clipping, rotation, scaling, adding noise, blurring, changing the shading or occlusion content, changes the original dataset from the pixel level, but it has little effect on the brain topology graph data. Because graph data focuses more on the

*Corresponding author

 tengyy@bmie.neu.edu.cn (Y. Teng)

structure information of graph, such as the clustering coefficient and local efficiency of nodes, correlation matrix, relevance and efficiency between two nodes, whether the nodes themselves form hub points and the rich-club between them, etc. At the beginning, people used the theory (Betzel et al., 2016; Vertes et al., 2012) of complex networks to construct or generate graphs with graph theory parameters similar to those in the real world, so that they also have scale-free, small world and other previously proven graph theory properties (Farahani et al., 2019; Rubinov and Sporns, 2010). However, because the mechanism of brain disease is not clear, the method of thinking that the patients with brain disease have similar graph attributes contains some subjectivity. On the contrary, many normal people have different brain structure attributes, which will cause great interference to our model of generating brain network.

Fortunately, in recent years, with the maturity of image data generation model (Braun et al., 2018; Grover and Leskovec, 2016; Leskovec et al., 2008), many excellent models for graph data generation have been built analogically, such as GraphVAE (Simonovsky and Komodakis), VGAE (Kipf and Welling, 2016), GraphGAN (Wang et al., 2017) and GraphRNN (You et al., 2018), etc. They have achieved good results on small graph datasets, such as proteins, citation networks, drug molecules, etc. Unfortunately, the existing discrimination methods are difficult to distinguish the differences between the generated graph and the real graph effectively and quantitatively (You et al., 2018). Many of them rely on the simple comparison of visual observation or statistical data (Simonovsky and Komodakis; Wang et al., 2017) (this is indeed feasible in the field of drug molecules and other small graphs).

Note that the existing graph generation models, such as GraphGAN (Wang et al., 2017) is implemented with Softmax when the generator estimates the connection distribution. Softmax function treats each node fairly and ignores the topological structure of brain network when it completes normalization. In GraphGAN, in order to add network information, the author proposes Graph Softmax (Wang et al., 2017) to calculate the estimated connection distribution, but the Softmax function with structure information needs to satisfy three conditions: In short, we need to satisfy a specific probability distribution, the connectivity probability of two vertices on the graph should decrease with the increase of the shortest distance, and the calculation of connectivity distribution should only cover a small number of nodes (such as the nodes close to v_c). Obviously, these conditions are not suitable for the study of brain networks. In addition, the limitation of GraphVAE is that the amount of computation is much larger than GraphRNN, and it is difficult to compute the graph with more nodes, such as brain network graph (You et al., 2018). We note that the original intention of RNN is to simulate the working mechanism and training process of some neurons in the human brain (Ahmadi and Tani, 2017; Idei et al.; Pellicano and Burr, 2012). Although we can't build as many neurons as the human brain, we hope to achieve better results for specific tasks. In recent years,

studies on the mechanism of brain dynamics have proved that RNN can be used to simulate the human brain (Güçlü and van Gerven, 2016).

So a natural idea is whether these models can be applied in the field of brain diseases, and whether the data generated is enough to replace the real-world brain graph (Braun et al., 2018; Zhao et al., 2020). Brain formation is also a new topic in recent years. Its ultimate goal and prospect are very promising. One of them is to simulate human brain development and predict brain diseases (Betzel et al., 2016; Braun et al., 2018; Chang et al., 2019; Kazi et al., 2018; Vertes et al., 2012). In recent years, Deep reinforcement learning (RL) has developed in depth and breadth in the mechanism of single brain mechanism (Botvinick et al., 2020). Moreover, due to the strong specificity of brain diseases such as Autism and many subtypes of patients, we hope to find a general method to eliminate a few differences among patients and train them to learn their common model.

We get inspiration from the generative teaching networks (GTNs) proposed by Such et al. (2019). This model generates completely artificial data to guide the model to have faster efficiency and learning speed. The model generates completely artificial graph data to guide the model to have faster learning speed. In order to further improve the accuracy of the model, we use GraphRNN to learn the edge connection distribution of patients and controls in the data generation step, and generate incentive data for the two types of data, so that the discrimination model has higher efficiency and accuracy.

So our final idea is to learn the distribution of brain networks in the real world based on GraphRNN, and then use it to generate incentive data to improve the identification ability of the original deep learning model.

2. Methodology

The existing datasets are preprocessed with MATLAB, and the optimal parameters such as atlas, threshold and preprocessing method are selected to make the subsequent experiments unaffected. Using the new dataset after processing, GraphRNN is allowed to learn the data of Autism and Control group respectively, and generate the dataset containing false Autism and Control. At the same time, the discrimination model used after training also selects the optimal parameters and model, and the model can be used to judge the quality of the previously generated dataset. Finally, the real brain network and the generated dataset are combined and disrupted, and the optimal discriminant model is trained to predict the real binary brain network dataset. Because it comes from the original dataset, it is essentially to extract the features of the ground truth data, and finally improve the existing model.

2.1. Data preprocessing

This paper refers to the work of Abraham et al. (2017) to solve how to extract times series to build a functional connectome. Because ABIDE(http://fcon_1000.projects.nitrc.org/indi/abide/) contains data from Caltech, CMU,

KKI and other 17 Organizations. In addition to the parameters we can control, such as TR, TE, Flip angle, Slices, there are also uncontrollable factors, such as Voxel size, Slice thickness, Participant instructions (e.g. eyes open vs. closed), Recruitment strategies (age-group, IQ-range, level of impairment, treatment history and acceptable comorbidities). This leads to the problem of heterogeneous graph which is difficult to avoid.

In previous studies (Anirudh and J. Thiagarajan, 2019; Choi, 2017; Eslami et al., 2019; Khosla et al., 2018; Kong et al., 2019; Ktena et al., 2018; Xia-An et al., 2018; Xinyu et al., 2017; Yao et al.), the brain graph data is usually the functional connectivity matrix between the set of brain region of interest (ROI). The data is based on the expert's examination results, excluding most of the largely incomplete brain coverage, high movement peaks, ghosting and other scanner artifacts. At the same time, preprocessing without deleting data is also carried out, which includes slice-timing correction, image realignment to correct for motion, and intensity normalization (Abraham et al., 2017; Ferrari et al., 2020). We keep some datasets which are still controversial in preprocessing methods for later discussion. In fact, through expert inspection data, these datasets have been smaller than the original dataset of 1112 subjects in varying degrees.

We used the same preprocessing pipeline (Craddock et al., 2013b) to ensure consistency with existing studies (Abraham et al., 2017; Ktena et al., 2018; Parisot et al.), which involves motion correction, slice timing correction, skull stripping and nuisance signal regression. Whether global mean intensity normalization and band-pass filtering (0.01-0.1Hz) is processed is currently controversial, so we will carry out experimental verification.

2.2. Brain network and problem definition

In this paper, regions of interests (ROIs) under different atlases are defined as network nodes (Craddock et al., 2012; Tzourio-Mazoyer et al., 2002), so that the corresponding graph data of the same brain under different atlases are also different, which provides more reference groups for the training and verification of the later model. At the same time, the edge of brain connection is crucial to comprehend the deep structure of graph and explain the similarity between eigenvectors (Dosenbach et al., 2010). Then, for the time series of any two network nodes X and Y , the Pearson correlation coefficient matrix (Formula. 1) between them can be obtained. In the experiment, we add a threshold to control the sparsity of the network (Rubinov and Sporns, 2010; Yu et al., 2020). If the threshold exceeds, it means that there is edge connection between the two nodes, otherwise, there is no edge connection. We can use the binary adjacency matrix to represent the relationship between a patient or a control brain network node (Fig. 1), and transform the resting-state fMRI time series data into the ground truth data needed for the later generation of the graph.

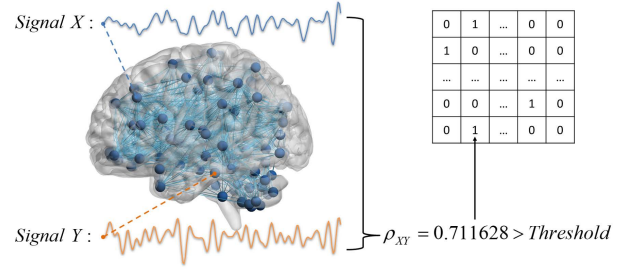


Figure 1: The edge connection of brain nodes is transformed into adjacency matrix under a specific threshold parameter.

$$\rho_{MN} = \frac{\sum_{i=1}^n (M_i - \bar{M})(N_i - \bar{N})}{\sqrt{\sum_{i=1}^n (M_i - \bar{M})^2} \sqrt{\sum_{i=1}^n (N_i - \bar{N})^2}} \quad (1)$$

After preprocessing, the brain network can be regarded as an undirected graph $G = (V, E)$, which is defined by the node set $V = \{v_1, v_2, \dots, v_n\}$ representing the ROIs and the definition of edge set $E = \{(v_i, v_j) | v_i, v_j \in V\}$ that represents the association between ROIs. Previously, we obtained its adjacency matrix by preprocessing. In fact, because the representation of adjacency matrix is not unique, we assume that the nodes selected under the specified brain region template have a sort, and map the nodes to the adjacency matrix. More precisely, $\{\psi(v_1), \psi(v_2), \dots, \psi(v_n)\}$ is the permutation of node set $\{v_1, v_2, \dots, v_n\}$.

We define Ψ the possible arrangement set of all brain network nodes (if the template has n brain regions, then Ψ has $n!$ arrangements). In the last part we get its adjacency matrix by preprocessing. Actually, for the same brain network graph, the adjacency matrix representation is not unique. Therefore, we need to determine in advance a set of appropriate ranking ψ of the selected nodes under the brain regions' mask, which is suitable for all patients and typical controls.

Then for the node arrangement under a group of brain area templates, the brain network G of patients or control group can be represented as a group $A^\psi \in \mathbb{R}^{n \times n}$, where $A_{i,j}^\psi \in \mathbb{1}[(\psi(v_i), \psi(v_j)) \in E]$. Note that in the adjacency matrix set, the elements of $A^\psi = \{A^\psi | \psi \in \Psi\}$ correspond to the same underlying brain network graph. Our goal of generating the model is to learn the distribution $p_{model}(G)$ of the existing data brain network from the brain observation graph data $\mathbb{G} = \{G_1, G_2, \dots, G_s\}$ sampled from the real world $p(G)$ (Fig. 2).

We assume that the order ψ of each brain node is equal probability, i.e., $p(\psi) = \frac{1}{n!}, \forall \psi \in \Psi$. Therefore, we want to use the existing brain graphs for augmentation. Because the traditional pixel level augmentation methods are not suitable for graphs, in fact, the generated brain graphs also have exponential representation, which is different from the previous generation models for images, texts and time series. In addition, the traditional method is generally single input training

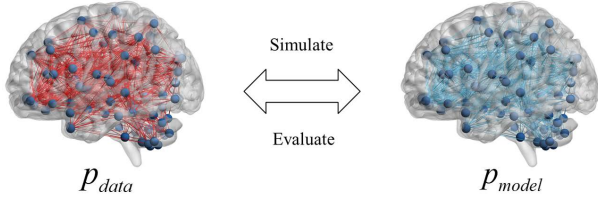


Figure 2: The purpose of training is to make the distribution of the model approximate to that of the real world brain network.

image, but the graph field can integrate multiple graphs into a large graph, and then use annotation to locate the features or labels of subgraphs.

2.3. GraphRNN: Deep generative models for brain network

The key idea of GraphRNN (You et al., 2018) is to represent graphs under different node orderings as sequences, and then to build an autoregressive generative model on these sequences. The advantage of this method is that it allows us to model large graphs with complex edge dependencies (such as the brain functional connectivity graph), which is not affected by the common shortcomings of other generation methods (such as GraphGAN (Wang et al., 2017) and GraphVAE (Simonovsky and Komodakis)). And GraphRNN can introduce the idea of breadth first search (BFS) node traversal to greatly reduce the complexity of all possible node sequence learning. In this autoregressive framework, the complexity of the model can be greatly reduced by sharing weights with recurrent neural networks (RNNs).

Fig. 3 shows the process of GraphRNN learning brain network step by step. The main idea is that we decompose graph generation into a process of generating a series of nodes (through graph level RNN), and the other process generates a series of edges (through edge level RNN) for each newly added node. Note that this is only a traversal method for learning the ground truth graph of the known real world. But for our trained model to generate new brain network nodes, it will help us to explore the mechanism of Autism, because most Autism is formed during the early brain development.

Graph is a complex data structure. In order to optimize graph operation, we first define the mapping f_S from graph to a sequence. For a graph $G \sim p(G)$ with n brain nodes in order ψ , we have

$$S^\psi = f_S(G, \psi) = (S_1^\psi, S_2^\psi, \dots, S_n^\psi) \quad (2)$$

where each element $S_i^\psi \in \{0, 1\}^{i-1}$, $i \in \{1, 2, \dots, n\}$ in the sequence is an adjacency vector representing the edges between brain network node $\psi(v_i)$ and the previous brain network nodes $\psi(v_j)$, $j \in \{1, 2, \dots, i-1\}$:

$$S_i^\psi = (A_{1,i}^\psi, A_{2,i}^\psi, \dots, A_{i-1,i}^\psi)^T, \forall i \in \{2, 3, \dots, n\} \quad (3)$$

We will not consider the self-connection within a certain brain region, so we prohibit self-loops and initialize S_1^ψ as an empty vector. For undirected brain graphs, S^ψ determines a

unique graph G . In this way, we transform the learning $p(G)$ which is difficult to define in the sample space into the observation value of S^ψ under the brain region mask sampling. Since S^ψ is a sequence, it can be modeled. Then the $p(G)$ of the whole graph can be transformed into:

$$p(G) = \sum_{S^\psi} p(S^\psi) \quad (4)$$

Where $p(S^\psi)$ is the distribution that we want to learn from the generative model. Due to the sequence property of S^ψ , we can further decompose $p(S^\psi)$ into the product of conditional distributions on each brain node:

$$p(S^\psi) = \prod_{i=1}^{n+1} p(S_i^\psi | S_1^\psi, \dots, S_{i-1}^\psi) \quad (5)$$

We will set S_{n+1}^ψ as end of sequence, and using $p(S_i^\psi | S_{<i}^\psi)$ to simplify $p(S_i^\psi | S_1^\psi, \dots, S_{i-1}^\psi)$.

It is observed that $p(S_i^\psi | S_{<i}^\psi)$ has to capture how the current node $\psi(v_i)$ links to the previous node based on the connection among the previous nodes, so RNN can be used to parameterize the distribution of $p(S_i^\psi | S_{<i}^\psi)$. In order to achieve a scalable model, the neural network can share the weight in all time steps i . The state transition function and output function of RNN can be expressed as:

$$\begin{aligned} h_i &= f_{trans}(h_{i-1}, S_i^\psi) \\ \theta_{i+1} &= f_{out}(h_i) \end{aligned} \quad (6)$$

Where $h_i \in \mathbb{R}^d$ is a vector encoding the state of the graph so far, S_i^ψ is the adjacency vector of the most recently generated node i , and θ_{i+1} specifies the adjacency vector distribution of the next node. Where S_i^ψ follows the arbitrary distribution $P_{\theta_{i+1}}$ of binary vectors.

The loss function of each time is defined as the binary cross entropy loss. Then the RNN model minimizes the following loss function:

$$L = -\frac{1}{N-1} \sum_{i=0}^{N-1} [y_i^* \log(y_i) + (1 - y_i^*) \log(1 - y_i)] \quad (7)$$

Where y_i^* is the corresponding value of binary matrix obtained by preprocessing, y_i is the output of RNN unit in each step, and N is the number of all possible connections, which is related to the number of nodes selected for brain mask.

3. Experiments

3.1. Datasets description and effect evaluation

The data support of this paper comes from the ABIDE dataset (Di Martino et al., 2014) of the preprocessed connectors project (PCP) (Craddock et al., 2013a), which is a public dataset of neuroimaging data from 539 patients and 573 controls. The whole dataset is provided by 16 institutions around the world (Abraham et al., 2017). In this experiment, resting state functional MRI (rs-fMRI) data was selected. In order to facilitate comparison with other studies,

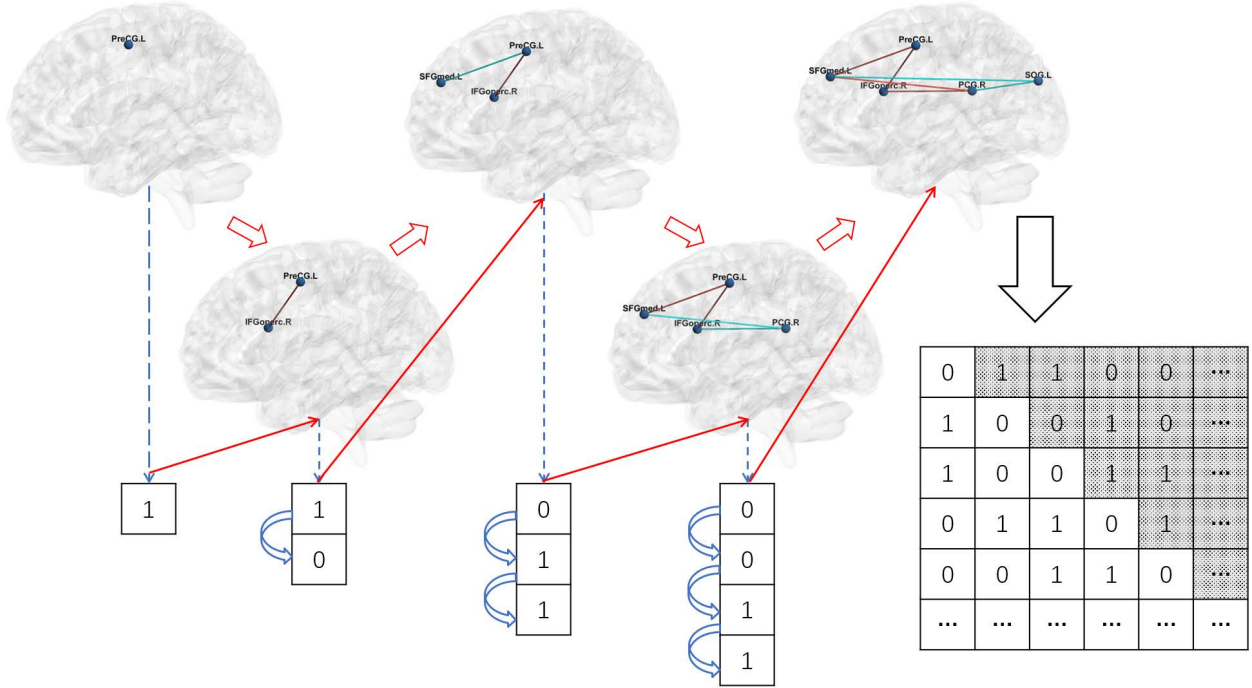


Figure 3: The process of brain network deduction by GraphRNN. The red arrows denote the graph level RNN that encodes the graph state vector h_i in its hidden state updated by the predicted adjacency vector S_i^w for $\psi(v_i)$. The blue arrows represent the edge level RNN whose hidden state is initialized by the graph level RNN used to predict the adjacency vector S_i^w for $\psi(v_i)$.

we selected the data processed by C-PAC (The Configurable Pipeline for the Analysis of Connectomes) (Craddock et al., 2013b). According to the research process of Abraham et al. (2017), we only keep the images whose average frame by frame displacement of the function image is less than 0.2, and the rest of the data that may have negative impact on the model results have been eliminated in the preprocessing.

For the part of data impact assessment, t-distributed stochastic neighbor embedding (t-SNE) is used to evaluate the dataset qualitatively and visually, and residual neural network (ResNet) is used as the classifier of the whole model for quantitative comparison. For other models, we use real-world brain datasets for pre-experimental classification, and reproduce the effect of graph neural network proposed in recent years. Unfortunately, it does not achieve better accuracy than ResNet. In order to control the influence of other factors and stabilize the model, the classifier is fixed.

There are two purposes for ResNet to quantify the classification effect by accuracy: One is to determine which preprocessing method is effective for model learning in the initial part of model training, so as to determine an appropriate preprocessing method and provide a more effective ground truth graph for generating model; the other is to provide a method to measure the quality of the generated graphs. Because the traditional measurement methods (histogram, PSNR, SSIM, NMI) are difficult to measure the quality of brain topology graph, and the distance index in graph theory is also difficult to measure the deep features. So we expect to use deep layer ResNet to detect the difference of the deep features between autistic patients and typical controls.

3.2. Defining nodes based on brain atlas

In the previous section, we use Formula. 1 to constructed the rules of the edge of brain network. The rules in this section are to make rules and experiments for nodes. Because the principle of using different atlas is different, we hope to find the impact of these atlases on the model. The four brain atlas regions selected in this paper are also collected through C-PAC:

- Automated Anatomical Labeling (AAL): The AAL atlas is based on Montreal Neurological Institute (MNI) regions drawn from T1 weighted images of a single subject. The main method is to segment the anatomical region manually, and then calibrate the program automatically. In this paper, we select the mask which contains 116 brain region nodes.
- Harvard-Oxford (HO): The HO atlas is a probability atlas. The T1 weighted image is affine transformed to MNI space by FSL, and then the transformation is applied to a single label. It was created by the FMRI analysis team in Oxford, UK. In this paper, we select the mask which contains 111 brain region nodes.
- Craddock 200 (CC200): The CC200 atlas refers to the research of Craddock et al. The principle of brain atlas formation through grey matter master is to use normalized cut and spectral clustering algorithm, and the final brain atlas has 200 brain region nodes.
- Craddock 400 (CC400): This brain atlas is an expanded version of cc200 with 400 brain region nodes.

The graph generated by different atlas for the same subject

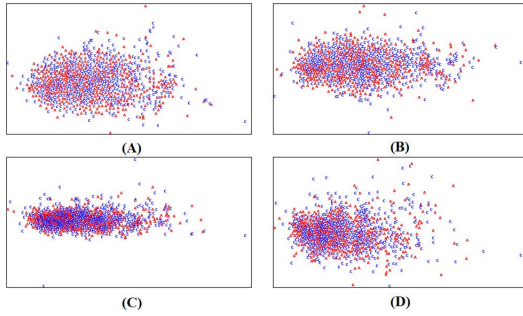


Figure 4: t-SNE is used to embed ABIDE dataset under different masks (A)AAL, (B)HO, (C)CC200, (D)CC400 into two-dimensional space for visualization, in which "A" represents autistic patients and "C" represents typical controls.

is heterogeneous, because the node structure and edge connection are different. In order to preliminarily estimate the advantages and disadvantages of these datasets, this paper uses t-distributed stochastic neighbor embedding (t-SNE) to reduce the dimension of the data set before the experiment, and then makes a qualitative analysis of the mask selection.

Due to the indeterminacy of data sources in band-pass filtering and global signal regression (Craddock et al., 2013a), in addition to the number of brain nodes directly affected by the template. Under the same threshold conditions, we conducted ablation experiments to determine whether the real data need filtering and global signal regression, so as to determine the effective preprocessing data source and generate data for the later model. We will carry out model learning (Table 1) according to the four kinds of data generated by the above preprocessing, and select the appropriate preprocessing strategy through the accuracy.

Fig. 4 reveals that ABIDE dataset is difficult to classify under each mask, which is consistent with the fact that most studies have low accuracy. Therefore, we optimize the dataset and use convolutional neural network to quantify the effect of the dataset. Since the accuracy of the model is relatively stable when filtering without global signal regression and using the AAL brain atlas with 116 nodes (Table 1), the above strategy is adopted in the later verification. But so far, we only select the appropriate dataset, and do not operate on the data, so we carry out further evaluation experiments to generate data learning and reinforce the original model, and then use ResNet to quantify the effect of the dataset.

3.3. Ablation experiment of model parameters

First of all, we conducted threshold selection experiments for single source real data. Based on the threshold of most previous research experiments, we took a group of larger values, a group of smaller values, a group of moderate values, and adaptive threshold based on Otsu method (the threshold determined by the maximum inter class variance) to compare with each other. The 50-layer ResNet model was used in the experiment. All the data were evaluated by AAL mask with 116 brain nodes. The number of edges depends on the threshold. The maximum number of edges is the original

Table 1

The four kinds of data generated by the above preprocessing.

Method	Mask	Accuracy(%)
Filter+Global	AAL116	61.80
	HO111	55.06
	CC200	52.87
	CC400	53.93
Filter	AAL116	68.53
	HO111	65.52
	CC200	59.55
	CC400	61.63
Global	AAL116	59.55
	HO111	59.55
	CC200	52.81
	CC400	57.30
/	AAL116	59.55
	HO111	55.68
	CC200	51.69
	CC400	57.30

* For the preprocessing method including global signal correction, the global mean signal includes interference variable regression. After variable regression, band-pass filter (0.01~0.1 Hz) was used.

matrix.

In order to verify whether the common reversing and triangular matrix in many studies have an impact on the model, we also reversed the brain connectivity network dataset under different threshold processing (that is, the edge connection is set to "0", the connection without edge is set to "1") and preserved the upper triangular matrix. Before the quantitative comparison experiment, we compared the datasets visually and qualitatively (Fig. 5). Finally, we put the original coefficient matrix into the model for comparison. The matrix is essentially a weight graph, and the edge (without considering the brain region self-connection) is formed between each node, and the weight of the edge represents the correlation coefficient of the average time series of the two brain regions. Table 2 shows the discrimination effect of these datasets under ResNet50.

Because there are too many edges, we choose the threshold=0.5 to reduce the number of edges, but the accuracy will not be significantly affected.

Considering the influence of classification model, we compare the influence of various ResNet and VGG on classification effect. In this way, we determine the ResNet discriminant model which can not only provide more effective ground truth graph for the generated model, but also measure the quality of the generated graphs. The specific step is to train and adjust the parameters of the original threshold dataset, and take the optimal discrimination ability of the model as the benchmark. Then, the generated model generates a nearly equal volume of Autism dataset and Control dataset (Fig. 6 is the visualization of the dataset). After eliminating the obvious failure and sparse data, the total data set

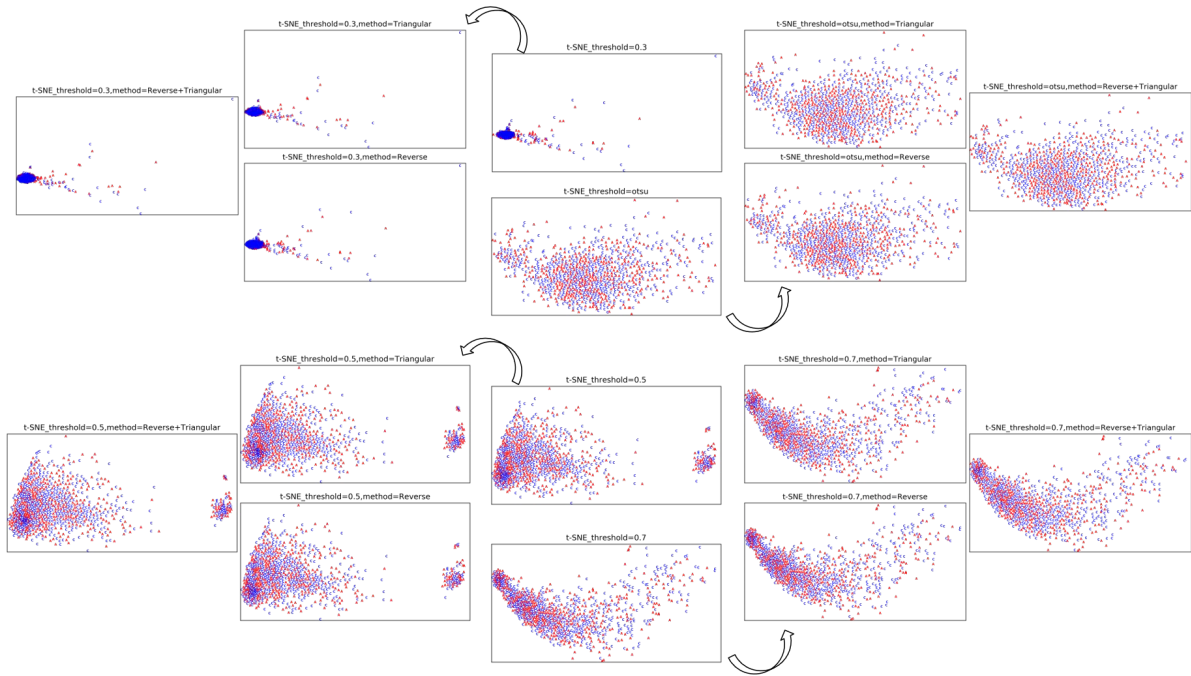


Figure 5: Using t-SNE to embed datasets of different thresholds and methods into two-dimensional space for qualitative comparison, other preprocessing methods almost have no effect on datasets, while the impact of threshold is very considerable.

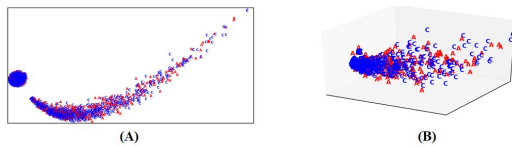


Figure 6: T-SNE is used to embed the generated dataset into (A)two-dimensional and (B)three-dimensional space for qualitative comparison.

capacity is 871 ± 10 . It does not change other parameters, and only uses the generated data to train the original different models. As an experiment to select discriminant model, the original brain network dataset is used to verify the effect of the trained model (Table 3).

In order to further verify the learning ability of the model trained by generate data in the third part, we will train and verify the testing dataset which is also a double label testing dataset of patients and controls according to the proportion of pre-training, the type of dataset and the proportion of testing dataset. It is excluded that the proportion of training dataset is too small or too large, which leads to the distortion of model verification effect (i.e. the ratio is about 0.1 or 0.9). In the process of pre-training, we notice that the model after pre-training with generated data can achieve good results when the ratio is 0.6 (Fig. 7, orange line). When the blank model used for control directly tests raw data without pre-training, the effect is rather unstable and the accuracy is relatively low (Fig. 7, blue line). The discrimination ability of the final model, no matter what proportion of validation, will be higher than that of the untrained control model (Fig. 7, green line). Therefore, we choose the best model

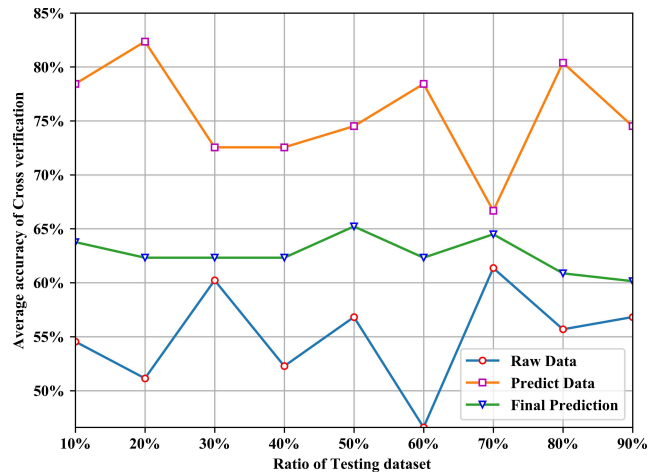


Figure 7: The comparison of the accuracy of the testing dataset divided by different proportions.

and proportion, i.e. pre-training Resnet-50 model with ratio of 0.6. We test the effect of the three datasets in Table 3 and adjust the test proportion to 0.1 for comparison (Fig. 8). Because the model pre-trains the generated data, the prediction of the generated dataset is much higher than that of other groups.

3.4. Comparative experiments of generating models with optimal parameters

According to the experimental results in the previous section, we select the optimal hyper-parameters and strategies for the dataset and model. Based on these, this paper compares the traditional degree based and clustering based

Table 2

The performance experiment of the ResNet50 model under the same atlas, different thresholds and preprocessing.

Threshold	Other preprocessing	Accuracy(%)	Number of Node	Number of Edge
0.3	/	52.28	A=46748 C=54288	A=1135985 C=1366380
	Reverse	56.81		
	Triangular	53.71		
	R+T	53.45		
0.5	/	60.80	A=46748 C=54288	A=432649 C=535424
	Reverse	58.27		
	Triangular	57.14		
	R+T	59.43		
0.7	/	52.13	A=46748 C=54288	A=74421 C=96445
	Reverse	52.21		
	Triangular	57.95		
	R+T	54.52		
Otsu threshold	/	54.41	A=46748 C=54288	A=1527691 C=1804461
	Reverse	58.09		
	Triangular	57.95		
	R+T	56.74		
Original	/	61.36	A=46748 C=54288	A=2688010 C=3121560

* A=Autism, C=Control, Reverse means to swap 0 and 1 in the graph, Triangular denotes Preserving the triangular matrix, Original uses the unprocessed Pearson correlation matrix.

** Note that we use the same model and model parameters here.

Table 3

The performance of raw data, generated data and Mixed data(raw + generated) training model to forecast raw data in different models.

Data used	Model	Accuracy(%)
Raw data training model to forecast raw data (threshold=0.5)	ResNet-18	54.66
	ResNet-34	58.30
	ResNet-50	60.80
	ResNet-101	52.61
	VGG16	52.27
Generated data training model to forecast raw data (threshold=0.5)	ResNet-18	71.93
	ResNet-34	74.09
	ResNet-50	76.48
	ResNet-101	71.25
	VGG16	51.71
Mixed data training model to forecast raw data(threshold=0.5)	ResNet-18	58.70
	ResNet-34	63.04
	ResNet-50	69.57
	ResNet-101	57.25
	VGG16	48.86

* VGG16 will be removed during validation because it performs poorly during training.

generation networks, as well as the comparative experiments using GraphRNN, GraphMLP and GraphVAE.

In the specific experiment, different generation models were used to learn the data of the original patients and the control group under the same threshold and other parameters under the optimal strategy of this experiment. For example, the GraphRNN after learning the real graph data, will

get a model GraphRNN-A to generate the brain network of Autism, and a model GraphRNN-C for Control. These models are then used to generate a set of generated datasets with the same number of samples, which are mixed into the original dataset to train ResNet50 discriminant model. Finally, the ResNet50 model is used to test the original data in the same ratio to evaluate the learning effect.

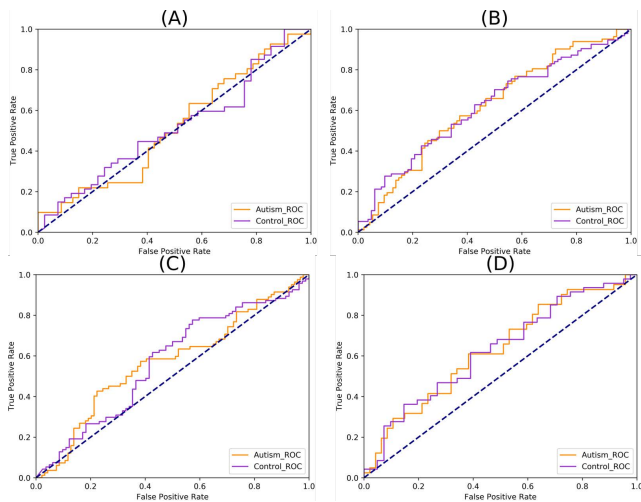


Figure 8: The ROC curves of patients and controls were predicted by generate data pre-training model. (A)Raw data training model to forecast raw data ratio=0.1; (B)Generate data training model to forecast raw data ratio=0.1; (C)Generate data training model to forecast raw data ratio=0.6; (D)Generate data training model to forecast raw data ratio=0.9.

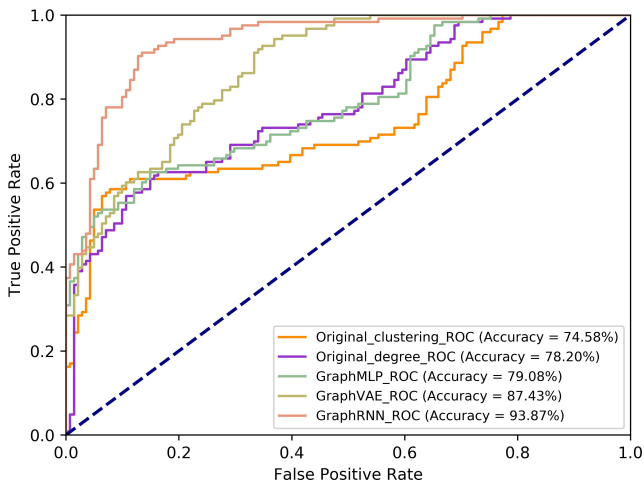


Figure 9: The ROC curves of control experiment was generated by different models with the same parameters in Autism.

After the cross validation of the original dataset not added to the generated data, we draw the ROC curves of the validation results of different generation models ((Fig. 9). It can be seen that due to the guidance and participation of the generated model, ResNet50 has significantly improved the accuracy (61.36%) of identifying the original ABIDE dataset that is not added to the generated data compared with the original ResNet50 model (Table 3) that is not reinforced by the generated data. The comparison results of different generation models show that GraphRNN is more prominent for the guidance model, which improves the accuracy of 32.51% compared with the previous ResNet50 model.

4. Results and discussion

Due to the high heterogeneity of Autism brain datasets, the difficulty of distinguishing brain network data features, the excessive number of graph edges, and the interference of other factors on the final generation and discrimination model, the accuracy of the data will decrease by 2.27% to 10.22% compared with the untreated original data, and the accuracy of some preprocessing methods will even differ by 16.84% under the same conditions. This study proves that the selection of preprocessing strategy in the early stage of brain formation model is particularly important for the effect of model discrimination.

The generated data is generated from the raw data, but in most of the training, using the same model, these data have a higher level of recognition, which is 16.24% to 25.02% higher than the raw data in different ResNet model. We speculate that in the model training, we constantly improve the probability that patients or controls may have edge connection, and set the unimportant factors to 0, resulting in the final generated graph features of patients and controls are more easily distinguished by the model.

In addition, it is noted that the reinforcement of generated data also improves the discrimination of ResNet model on the original ABIDE dataset. The most significant effect is the 50-layer ResNet, and the best generation model is GraphRNN, which improves the accuracy by 32.51% compared with the model reference experiment without generation data reinforcement. It might be that the data model distribution is learned in advance, which makes the model more inclined to extract the features with high edge connection probability in the generated model training (Battaglia et al., 2018), so it is also a good pre-training method in essence.

Although the pre-training of GraphRNN generation makes the model achieve good results, there is still no way to deal with the brain network formed at pixel level due to too many edges and nodes. In addition, the interaction ability of discriminator to generator is weak, and the principle of generating data depends on brain function connection matrix to a great extent. In the future work, we will further optimize the generating unit so that the model can accommodate more detailed graphs. And it will increase the guidance of discriminator to the generator, making the generator produce better brain network.

Acknowledge

This work was supported by the Fundamental Research Funds for the Central Universities.(N2019006 and N180719020)

References

- Abraham, A., Milham, M.P., Di Martino, A., Craddock, R.C., Samaras, D., Thirion, B., Varoquaux, G., 2017. Deriving reproducible biomarkers from multi-site resting-state data: An autism-based example. *Neuroimage* 147, 736–745. URL: <https://www.ncbi.nlm.nih.gov/pubmed/27865923>, doi:10.1016/j.neuroimage.2016.10.045.
- Ahmadi, A., Tani, J., 2017. Bridging the Gap Between Probabilistic and Deterministic Models: A Simulation Study on a Variational Bayes

- Predictive Coding Recurrent Neural Network Model. doi:10.1007/978-3-319-70090-8_77.
- Anderson, J.S., Druzgal, T.J., Froehlich, A., DuBray, M.B., Lange, N., Alexander, A.L., Abildskov, T., Nielsen, J.A., Cariello, A.N., Cooper, J.R., Bigler, E.D., Lainhart, J.E., 2011. Decreased inter-hemispheric functional connectivity in autism. *Cerebral Cortex* 21, 1134–1146. URL: <https://doi.org/10.1093/cercor/bhq190>, doi:10.1093/cercor/bhq190.
- Anirudh, R., J. Thiagarajan, J., 2019. Bootstrapping Graph Convolutional Neural Networks for Autism Spectrum Disorder Classification. doi:10.1109/ICASSP.2019.8683547.
- Battaglia, P.W., Hamrick, J.B., Bapst, V., Sanchez-Gonzalez, A., Zambaldi, V., Malinowski, M., Tacchetti, A., Raposo, D., Santoro, A., Faulkner, R., Gulcehre, C., Song, F., Ballard, A., Gilmer, J., Dahl, G., Vaswani, A., Allen, K., Nash, C., Langston, V., Dyer, C., Heess, N., Wierstra, D., Kohli, P., Botvinick, M., Vinyals, O., Li, Y., Pascanu, R., 2018. Relational inductive biases, deep learning, and graph networks. arXiv:1806.01261.
- Betzel, R.F., Avena-Koenigsberger, A., Goni, J., He, Y., de Reus, M.A., Griffa, A., Vertes, P.E., Misis, B., Thiran, J.P., Hagmann, P., van den Heuvel, M., Zuo, X.N., Bullmore, E.T., Sporns, O., 2016. Generative models of the human connectome. *Neuroimage* 124, 1054–1064. URL: <https://www.ncbi.nlm.nih.gov/pubmed/26427642>, doi:10.1016/j.neuroimage.2015.09.041.
- Botvinick, M., Wang, J.X., Dabney, W., Miller, K.J., Kurth-Nelson, Z., 2020. Deep reinforcement learning and its neuroscientific implications. *Neuron* 107, 603–616. URL: <https://www.ncbi.nlm.nih.gov/pubmed/32663439>, doi:10.1016/j.neuron.2020.06.014.
- Braun, U., Schaefer, A., Betzel, R.F., Tost, H., Meyer-Lindenberg, A., Bassett, D.S., 2018. From maps to multi-dimensional network mechanisms of mental disorders. *Neuron* 97, 14–31. URL: <http://www.sciencedirect.com/science/article/pii/S0896627317310358>, doi:https://doi.org/10.1016/j.neuron.2017.11.007.
- Chang, K., Beers, A.L., Bai, H.X., Brown, J.M., Ly, K.I., Li, X., Senders, J.T., Kavouridis, V.K., Boaro, A., Su, C., Bi, W.L., Rapalino, O., Liao, W., Shen, Q., Zhou, H., Xiao, B., Wang, Y., Zhang, P.J., Pinho, M.C., Wen, P.Y., Batchelor, T.T., Boxerman, J.L., Arnaout, O., Rosen, B.R., Gerstner, E.R., Yang, L., Huang, R.Y., Kalpathy-Cramer, J., 2019. Automatic assessment of glioma burden: a deep learning algorithm for fully automated volumetric and bidimensional measurement. *Neuro Oncol* 21, 1412–1422. URL: <https://www.ncbi.nlm.nih.gov/pubmed/31190077>, doi:10.1093/neuonc/noz106.
- Choi, H., 2017. Functional connectivity patterns of autism spectrum disorder identified by deep feature learning. CoRR abs/1707.07932. URL: <http://arxiv.org/abs/1707.07932>, arXiv:1707.07932.
- Choi, H., Ha, S., Im, H.J., Paek, S.H., Lee, D.S., 2017. Refining diagnosis of parkinson's disease with deep learning-based interpretation of dopamine transporter imaging. *NeuroImage: Clinical* 16, 586–594. URL: <https://www.sciencedirect.com/science/article/pii/S2213158217302243>, doi:https://doi.org/10.1016/j.nicl.2017.09.010.
- Craddock, C., Benhajali, Y., Carlton, C., Francois, C., Evans, A., Jakab, A., Khundrakpam, B., Lewis, J., Qingyang, I., Michael, M., Chaogan, Y., Bellec, P., 2013a. The neuro bureau preprocessing initiative: open sharing of preprocessed neuroimaging data and derivatives. *Frontiers in Neuroinformatics* 7. doi:10.3389/conf.fninf.2013.09.00041.
- Craddock, C., James, A., Holtzheimer, P., Hu, X., Mayberg, H., 2012. A whole brain fmri atlas generated via spatially constrained spectral clustering. *Human brain mapping* 33, 1914–28. doi:10.1002/hbm.21333.
- Craddock, C., Sharad, S., Brian, C., Ranjeet, K., Satrajit, G., Chaogan, Y., Qingyang, I., Daniel, L., Vogelstein, J., Burns, R., Stanley, C., Mennes, M., Clare, K., Adriana, D., Castellanos, F., Michael, M., 2013b. Towards automated analysis of connectomes: The configurable pipeline for the analysis of connectomes (c-pac). *Frontiers in Neuroinformatics* 7. doi:10.3389/conf.fninf.2013.09.00042.
- Di Martino, A., Yan, C.G., Li, Q., Denio, E., Castellanos, F.X., Alaerts, K., Anderson, J.S., Assaf, M., Bookheimer, S.Y., Dapretto, M., Deen, B., Delmonte, S., Dinstein, I., Ertl-Wagner, B., Fair, D.A., Gallagher, L., Kennedy, D.P., Keown, C.L., Keyzers, C., Lainhart, J.E., Lord, C., Luna, B., Menon, V., Minshew, N.J., Monk, C.S., Mueller, S., Müller, R.A., Nebel, M.B., Nigg, J.T., O'Hearn, K., Pelphrey, K.A., Peltier, S.J., Rudie, J.D., Sunaert, S., Thioux, M., Tyszka, J.M., Uddin, L.Q., Vervaeke, J.S., Wenderoth, N., Wiggins, J.L., Mostofsky, S.H., Milham, M.P., 2014. The autism brain imaging data exchange: towards a large-scale evaluation of the intrinsic brain architecture in autism. *Molecular Psychiatry* 19, 659–667. URL: <https://doi.org/10.1038/mp.2013.78>, doi:10.1038/mp.2013.78.
- Dosenbach, N.U.F., Nardos, B., Cohen, A.L., Fair, D.A., Power, J.D., Church, J.A., Nelson, S.M., Wig, G.S., Vogel, A.C., Lessov-Schlaggar, C.N., Barnes, K.A., Dubis, J.W., Feczko, E., Coalson, R.S., Pruett, J.R., Barch, D.M., Petersen, S.E., Schlaggar, B.L., 2010. Prediction of individual brain maturity using fmri. *Science* 329, 1358. URL: <http://science.sciencemag.org/content/329/5997/1358.abstract>, doi:10.1126/science.1194144.
- Dvornek, N.C., Ventola, P., Pelphrey, K.A., Duncan, J.S., . Identifying autism from resting-state fmri using long short-term memory networks, in: *Machine Learning in Medical Imaging*, Springer International Publishing. pp. 362–370.
- Eslami, T., Mirjalili, V., Fong, A., Laird, A.R., Saeed, F., 2019. Asd-diagnet: A hybrid learning approach for detection of autism spectrum disorder using fmri data. *Frontiers in Neuroinformatics* 13. URL: <GotoISI>://WOS:000502132500001, doi:ARTN7010.3389/fninf.2019.00070.
- Farahani, F.V., Karwowski, W., Lighthall, N.R., 2019. Application of graph theory for identifying connectivity patterns in human brain networks: A systematic review. *Front Neurosci* 13, 585. URL: <https://www.ncbi.nlm.nih.gov/pubmed/31249501>, doi:10.3389/fnins.2019.00585.
- Ferrari, E., Bosco, P., Calderoni, S., Oliva, P., Palumbo, L., Spera, G., Fantacci, M.E., Retico, A., 2020. Dealing with confounders and outliers in classification medical studies: The autism spectrum disorders case study. *Artif Intell Med* 108, 101926. URL: <https://www.ncbi.nlm.nih.gov/pubmed/32972657>, doi:10.1016/j.artmed.2020.101926.
- Frith, C., 2004. Is autism a disconnection disorder? *The Lancet Neurology* 3, 577. URL: <https://www.sciencedirect.com/science/article/pii/S1474442204008750>, doi:https://doi.org/10.1016/S1474-4422(04)00875-0.
- Grover, A., Leskovec, J., 2016. node2vec: Scalable feature learning for networks. KDD:proceedings. International Conference on Knowledge Discovery & Data Mining , 855–864URL: <https://europepmc.org/articles/PMC5108654>, doi:10.1145/2939672.2939754.
- Güçlü, U., van Gerven, M., 2016. Modeling the dynamics of human brain activity with recurrent neural networks. *Frontiers in Computational Neuroscience* 11. doi:10.3389/fncom.2017.00007.
- Hahamy, A., Behrmann, M., Malach, R., 2015. The idiosyncratic brain: distortion of spontaneous connectivity patterns in autism spectrum disorder. *Nature Neuroscience* 18, 302–309. URL: <https://doi.org/10.1038/nn.3919>, doi:10.1038/nn.3919.
- Heinsfeld, A.S., Franco, A.R., Craddock, R.C., Buchweitz, A., Meneguzzi, F., 2018. Identification of autism spectrum disorder using deep learning and the abide dataset. *Neuroimage Clin* 17, 16–23. URL: <https://www.ncbi.nlm.nih.gov/pubmed/29034163>, doi:10.1016/j.nicl.2017.08.017.
- Idei, H., Murata, S., Chen, Y., Yamashita, Y., Tani, J., Ogata, T., . Reduced behavioral flexibility by aberrant sensory precision in autism spectrum disorder: A neurobotics experiment, in: 2017 Joint IEEE International Conference on Development and Learning and Epigenetic Robotics (ICDL-EpiRob), pp. 271–276. doi:10.1109/DEVLRN.2017.8329817.
- Just, M., Cherkassky, V., Keller, T., Minshew, N., 2004. Cortical activation and synchronization during sentence comprehension in high-functioning autism: Evidence of underconnectivity. *Brain : a journal of neurology* 127, 1811–21. doi:10.1093/brain/awh199.
- Kazi, A., Shekarforoush, S., Sridhar, A., Burwinkel, H., Vivar, G., Kortüm, K., Ahmadi, S.A., Albarqouni, S., Navab, N., 2018. InceptionGCN : Receptive Field Aware Graph Convolutional Network for Disease Prediction.
- Keown, C.L., Shih, P., Nair, A., Peterson, N., Mulvey, M.E., Müller, R.A., 2013. Local functional overconnectivity in posterior brain regions is associated with symptom severity in autism spectrum disorders. *Cell Reports* 5, 567–572. URL: <https://www.sciencedirect.com/science/>

- article/pii/S221112471300572X, doi:https://doi.org/10.1016/j.celrep.2013.10.003.
- Khosla, M., Jamison, K., Kuceyeski, A., Sabuncu, M.R., 2018. 3d convolutional neural networks for classification of functional connectomes. *Deep Learning in Medical Image Analysis and Multimodal Learning for Clinical Decision Support, Dlmia 2018* 11045, 137–145. URL: <GotoISI>://WOS:000477761800016, doi:10.1007/978-3-030-00889-5_16.
- Kipf, T.N., Welling, M., 2016. Variational graph auto-encoders. *NIPS Workshop on Bayesian Deep Learning*.
- Kong, Y.Z., Gao, J.L., Xu, Y.P., Pan, Y., Wang, J.X., Liu, J., 2019. Classification of autism spectrum disorder by combining brain connectivity and deep neural network classifier. *Neurocomputing* 324, 63–68. URL: <GotoISI>://WOS:000449368400008, doi:10.1016/j.neucom.2018.04.080.
- Ktena, S.I., Parisot, S., Ferrante, E., Rajchl, M., Lee, M., Glocker, B., Rueckert, D., 2018. Metric learning with spectral graph convolutions on brain connectivity networks. *Neuroimage* 169, 431–442. URL: https://www.ncbi.nlm.nih.gov/pubmed/29278772, doi:10.1016/j.neuroimage.2017.12.052.
- Lanillos, P., Oliva, D., Philippsen, A., Yamashita, Y., Nagai, Y., Cheng, G., 2020. A review on neural network models of schizophrenia and autism spectrum disorder. *Neural Networks* 122, 338–363. URL: http://www.sciencedirect.com/science/article/pii/S0893608019303363, doi:https://doi.org/10.1016/j.neunet.2019.10.014.
- Lawson, R., Rees, G., Friston, K., 2014. An aberrant precision account of autism. *Frontiers in human neuroscience* 8, 302. doi:10.3389/fnhum.2014.00302.
- Leskovec, J., Chakrabarti, D., Kleinberg, J., Faloutsos, C., Ghahramani, Z., 2008. Kronecker graphs: An approach to modeling networks. *Journal of Machine Learning Research* 11. doi:10.1145/1756006.1756039.
- Li, H., Parikh, N.A., He, L., 2018. A novel transfer learning approach to enhance deep neural network classification of brain functional connectomes. *Frontiers in Neuroscience* 12. URL: https://www.frontiersin.org/article/10.3389/fnins.2018.00491, doi:10.3389/fnins.2018.00491.
- Liu, M., Zhang, J., Adeli, E., Shen, D., 2018. Landmark-based deep multi-instance learning for brain disease diagnosis. *Medical Image Analysis* 43, 157–168. URL: https://www.sciencedirect.com/science/article/pii/S1361841517301524, doi:https://doi.org/10.1016/j.media.2017.10.005.
- Lu, D., Popuri, K., Ding, G.W., Balachandar, R., Beg, M.F., 2018. Multiscale deep neural network based analysis of fdg-pet images for the early diagnosis of alzheimer's disease. *Medical Image Analysis* 46, 26–34. URL: https://www.sciencedirect.com/science/article/pii/S1361841518300276, doi:https://doi.org/10.1016/j.media.2018.02.002.
- Marek, K., Jennings, D., Lasch, S., Siderowf, A., Tanner, C., Simuni, T., Coffey, C., Kiebertz, K., Flagg, E., Chowdhury, S., Poewe, W., Mollenhauer, B., Klinik, P.E., Sherer, T., Frasier, M., Meunier, C., Rudolph, A., Casaceli, C., Seibyl, J., Taylor, P., 2011. The parkinson progression marker initiative (ppmi). *Progress in Neurobiology* 95, 629–635. doi:10.1016/j.pneurobio.2011.09.005.
- Martínez-Murcia, F.J., Ortiz, A., Górriz, J.M., Ramírez, J., Segovia, F., Salas-Gonzalez, D., Castillo-Barnes, D., Illán, I.A., . A 3d convolutional neural network approach for the diagnosis of parkinson's disease, in: Ferrández Vicente, J.M., Álvarez Sánchez, J.R., de la Paz López, F., Toledo Moreo, J., Adeli, H. (Eds.), *Natural and Artificial Computation for Biomedicine and Neuroscience*, Springer International Publishing. pp. 324–333.
- Parisot, S., Ktena, S.I., Ferrante, E., Lee, M., Moreno, R.G., Glocker, B., Rueckert, D., . Spectral graph convolutions for population-based disease prediction, in: *Medical Image Computing and Computer Assisted Intervention; MICCAI 2017*, Springer International Publishing. pp. 177–185.
- Pellicano, E., Burr, D., 2012. When the world becomes 'too real': A bayesian explanation of autistic perception. *Trends in cognitive sciences* 16, 504–10. doi:10.1016/j.tics.2012.08.009.
- Petersen, R., Aisen, P.S., Beckett, L.A., Donohue, M., Gamst, A.C., Harvey, D.J., Jack, C., Jagust, W.J., Shaw, L., Toga, A.W., Trojanowski, J.Q., Weiner, M., 2010. Alzheimer's disease neuroimaging initiative (adni): Clinical characterization. *Neurology* 74, 201–9. doi:10.1212/WNL.0b013e3181cb3e25.
- Rubinov, M., Sporns, O., 2010. Complex network measures of brain connectivity: Uses and interpretations. *NeuroImage* 52, 1059–1069. URL: https://www.sciencedirect.com/science/article/pii/S105381190901074X, doi:https://doi.org/10.1016/j.neuroimage.2009.10.003.
- Shorten, C., Khoshgoftaar, T., 2019. A survey on image data augmentation for deep learning. *Journal of Big Data* 6. doi:10.1186/s40537-019-0197-0.
- Simonovsky, M., Komodakis, N., . Graphvae: Towards generation of small graphs using variational autoencoders, in: *Artificial Neural Networks and Machine Learning – ICANN 2018*, Springer International Publishing. pp. 412–422.
- Sivaranjini, S., Sujatha, C.M., 2020. Deep learning based diagnosis of parkinson's disease using convolutional neural network. *Multimedia Tools and Applications* 79, 15467–15479. URL: https://doi.org/10.1007/s11042-019-7469-8, doi:10.1007/s11042-019-7469-8.
- Such, F., Rawal, A., Lehman, J., Stanley, K., Clune, J., 2019. Generative Teaching Networks: Accelerating Neural Architecture Search by Learning to Generate Synthetic Training Data.
- Suk, H.I., Lee, S.W., Shen, D., The Alzheimer's Disease Neuroimaging, I., 2015. Latent feature representation with stacked auto-encoder for ad/mci diagnosis. *Brain Structure and Function* 220, 841–859. URL: https://doi.org/10.1007/s00429-013-0687-3, doi:10.1007/s00429-013-0687-3.
- Supekar, K., Uddin, L.Q., Khouzam, A., Phillips, J., Gaillard, W.D., Kenworthy, L.E., Yerys, B.E., Vaidya, C.J., Menon, V., 2013. Brain hyperconnectivity in children with autism and its links to social deficits. *Cell Reports* 5, 738–747. URL: https://www.sciencedirect.com/science/article/pii/S2211124713005706, doi:https://doi.org/10.1016/j.celrep.2013.10.001.
- Tzourio-Mazoyer, N., Landeau, B., Papathanassiou, D., Crivello, F., Etard, O., Delcroix, N., Mazoyer, B., Joliot, M., 2002. Automated anatomical labeling of activations in spm using a macroscopic anatomical parcellation of the mni mri single-subject brain. *NeuroImage* 15, 273–289. URL: https://www.sciencedirect.com/science/article/pii/S1053811901909784, doi:https://doi.org/10.1006/nimg.2001.0978.
- Vertes, P.E., Alexander-Bloch, A.F., Gogtay, N., Giedd, J.N., Rapoport, J.L., Bullmore, E.T., 2012. Simple models of human brain functional networks. *Proc Natl Acad Sci U S A* 109, 5868–73. URL: https://www.ncbi.nlm.nih.gov/pubmed/22467830, doi:10.1073/pnas.1111738109.
- Wang, H., Wang, J., Wang, J., Zhao, M., Zhang, W., Zhang, F., Xie, X., Guo, M., 2017. Graphgan: Graph representation learning with generative adversarial nets. *IEEE Transactions on Knowledge and Data Engineering PP*. doi:10.1109/TKDE.2019.2961882.
- Xia-An, B., Yingchao, L., Qin, J., Qing, S., Qi, S., Jianhua, D., 2018. The diagnosis of autism spectrum disorder based on the random neural network cluster. *Frontiers in Human Neuroscience* 12, 257.
- Xinyu, G., Dominick, K.C., Minai, A.A., Hailong, L., Erickson, C.A., Lu, L.J., 2017. Diagnosing autism spectrum disorder from brain resting-state functional connectivity patterns using a deep neural network with a novel feature selection method. *Frontiers in Neuroence* 11, 460.
- Yao, D., Liu, M., Wang, M., Lian, C., Wei, J., Sun, L., Sui, J., Shen, D., . Triplet graph convolutional network for multi-scale analysis of functional connectivity using functional mri, in: Zhang, D., Zhou, L., Jie, B., Liu, M. (Eds.), *Graph Learning in Medical Imaging*, Springer International Publishing. pp. 70–78.
- You, J., Ying, R., Ren, X., Hamilton, W.L., Leskovec, J., 2018. Graphrnn: A deep generative model for graphs. *arXiv:1802.08773*.
- Yu, Z., Qin, J., Xiong, X., Xu, F., Wang, J., Hou, F., Yang, A., 2020. Abnormal topology of brain functional networks in unipolar depression and bipolar disorder using optimal graph thresholding. *Prog Neuropsychopharmacol Biol Psychiatry* 96, 109758. URL: https://www.ncbi.nlm.nih.gov/pubmed/31493423, doi:10.1016/j.pnpbp.2019.109758.
- Zhang, L., Wang, M., Liu, M., Zhang, D., 2020. A survey on deep learning for neuroimaging-based brain disorder analysis. *Front Neurosci* 14, 779. URL: https://www.ncbi.nlm.nih.gov/pubmed/33117114, doi:10.3389/fnins.2020.00779.
- Zhao, A., Balakrishnan, G., Durand, F., Guttag, J.V., Dalca, A.V., . Data augmentation using learned transformations for one-shot medical image segmentation, in: *2019 IEEE/CVF Conference on Computer Vision and*

Pattern Recognition (CVPR), pp. 8535–8545. doi:10.1109/CVPR.2019.00874.

Zhao, T., Liu, Y., Neves, L., Woodford, O., Jiang, M., Shah, N., 2020. Data Augmentation for Graph Neural Networks.

Zoph, B., Cubuk, E., Ghiasi, G., Lin, T.Y., Shlens, J., Le, Q., 2019. Learning Data Augmentation Strategies for Object Detection.